Measurements of the total atomic differential cross section of elastic scattering of 59.54-keV photons

E. Casnati, C. Baraldi, and A. Tartari
Dipartimento di Fisica dell'Università, I-44100 Ferrara, Italy
(Received 20 March 1990)

Accurate measurements, mostly to within 2%, of the total atomic cross section for the elastic scattering of 59.54-keV photons on atoms in the $13 \leq Z \leq 82$ range were carried out at 60°, 90°, and 120° scattering angles. Very good agreement with other experimental data was observed, in particular, with those of Schumacher and Stoffregen [Z. Phys. A **283**, 15 (1977)]. The comparison with the theoretical results given by Kissel and co-workers [Phys. Rev. A **22**, 1979 (1980); Phys. Rep. **140**, 75 (1986)] confirms the validity of their procedure within the value intervals explored.

I. INTRODUCTION

In the past the amplitude of photons scattered coherently by atomic electrons, i.e., Rayleigh scattering, was calculated by different approaches depending on photon energy, atomic number, atomic shell, and scattering angle. Over limited intervals of these parameters, numerical methods of solution of the scattering matrix were employed which, although within an independent-electron model, included the important effects due to binding in intermediate states. However, the values included in today's extended tabulations of the coherent scattering cross section of photons by atomic electrons is based on the approximation of the nonrelativistic form factor,[1] of the relativistic form factor,[2] or of the relativistic modified form factor.[3] In the last decade Kissel *et al.*,[4] Kissel,[5] Kissel and Pratt,[6] and Kane *et al.*[7] established a procedure that makes it possible to obtain very accurate, to within 2%, Rayleigh cross-section values by combining the numerical evaluations of the scattering matrix for the innermost atomic shells with the modified atomic form factor for the real part, and the scale factor provided by the optical theorem for the imaginary part of the amplitudes due to the other shells. In order to facilitate comparison with experimental results, the same authors decided to include in their tabulated values the contributions other interactions (i.e., the nuclear Thomson and resonance scattering and Delbrück scattering) make to the amplitude of the photons elastically scattered by atoms. Such tabulations[7] include ten elements in the interval $13 \leq Z \leq 82$, seven typical photon energies between 59.54 keV and 1.33 MeV and cover 55 angles suitably spaced to simplify interpolations.

A correct evaluation of the contribution each atomic shell makes to the amplitude of elastically scattered radiation is of interest in various areas of basic knowledge, e.g., in studies on both solids and nuclei structure and in the experimental determination of the Delbrück scattering cross section. Also, in applied physics, an adequate estimate of the Rayleigh scattering cross section is useful: in plasma diagnostics and in astrophysics, for instance, where the performance of detectors during experiments must be appropriately predicted; in the calculations of the attenuation coefficients of narrow photon beams of wide medical and technological use, in analysis of the level of bone mineralization, as suggested by Bradley and Ghose.[8]

In practice, below 100 keV, Rayleigh interaction is the only process contributing to the atomic elastic scattering of photons. Therefore, the decision was made to carry out measurements in this region of energy, precisely at 59.54 keV, the results of which should have uncertainties comparable with those of the best theoretical values such as those calculated using the method of Kissel and coworkers.[4-7] At this photon energy, experimental data have already been gathered by Schumacher and Stoffregen,[9] Eichler and de Barros,[10] Smend and Czerwinski,[11] Nandi *et al.*,[12] Bui and Milazzo,[13] and Varier and Unnikrishnan.[14] However, such values present some dispersion, even though they are generally consistent within their uncertainties.

II. MEASUREMENT PRINCIPLES

The aim of obtaining accurate and precise results suggested the choice of the simplest geometrical arrangement, i.e., the reflection geometry with both source and detector endowed with collimators. The axes of these collimators, i.e., the axes of the incident and the observed beams, made the same angle with the normal to the scattering foil as in optical reflection. Moreover, the distances between source and scatterer and between scatterer and detector were equal in practice and very large in comparison with the dimensions of the scattering surface seen by the detector, and thus this surface practically belonged to a constant-scattering-angle surface.[15] The surface of revolution practice (Bradley and Ghose[16]) was ruled out because it was inappropriate for the use of the goniometric bench on which the source head, scatterer, and detector were placed in order to facilitate the repetition of measurements under the same scattering angle. Of course, the geometric arrangement chosen demanded long measuring times (from two to five days) to reach satisfactory counting statistics, but the electronic system

was assisted by a double-peak stabilizer and, as measuring time grew, the checks never showed a decrease in resolution under the controlled conditions of temperature and humidity in the irradiation room. The collimators of both source and detector were of the multivane type and were built by combining different materials in order to minimize the scattered and characteristic radiation arising inside them, which would be registered by the detector. The dimensions and alignment of the collimators were such that all the points of the scatterer seen by the detector were illuminated by the whole radiation source, and the solid angle under which the points of the scatterer "saw" the aperture of the vane closest to the detector was very small. The scheme of the experimental arrangement is given in Fig. 1.

With such an arrangement, and under the abovementioned conditions, if the intersection of the axes of the two collimators on the surface of the scatterer T is assumed as the reference point O, it is easy to show that, when the attenuation of air is neglected and the source is very small, the flux of radiation scattered by the detector through j-type interactions is given by

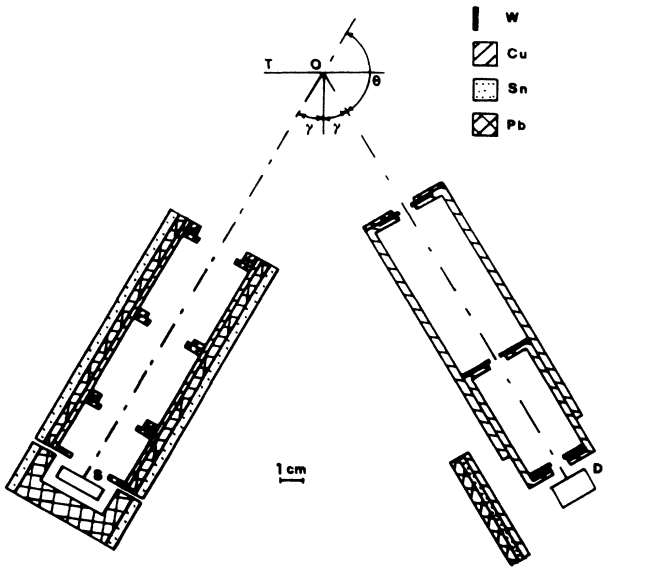

FIG. 1. Schematic layout of the experimental arrangement: S, source; D, detector; T, scatterer.

$$\Phi_u = 2n\varphi\Omega\sigma'_j hk^2(\cos\gamma)\int_0^L \exp[-(\mu_i+\mu_e)l/\cos\gamma]dl \times \int_{-r}^{r} \frac{(h+z\tan\gamma)(r^2-z^2)^{1/2}}{\{h(k\cos\gamma+l\cos 2\gamma)+z\tan\gamma[(h+k)\cos\gamma+l(1+\cos 2\gamma)]\}^2}dz \ . \quad (1)$$

In this expression γ is the angle of incidence and of reflection with respect to the normal at O to the scatterer and it is connected to the scattering angle θ by $\theta=\pi-2\gamma$; k and h are, respectively, the distances of O from the source and from the collimator vane closest to detector; r is the radius of the circle described by the intersection of the viewing cone with the plane through O and orthogonal to the axis of the collimator of the detector; L is the thickness of the scatterer, and n the number of atoms per its unit of volume; μ_i and μ_e are the attenuation coefficients of the radiation incident on and emerging from the scattering foil, respectively; φ is the incident flux density in O and Ω the solid angle under which the aperture of the vane closest to the detector is seen from O; $\sigma'_j=d\sigma_j/d\Omega$ is the differential cross section of the interactions of type j between photons and atoms. Keeping in mind that $l \ll h$, expression (1) can be approximated, well below the limit of the uncertainty accepted for the results, by the simpler expression

$$\Phi_u = 2n\varphi\Omega\sigma'_j hk^2 \frac{1-\exp[-(\mu_i+\mu_e)L/\cos\gamma]}{\mu_i+\mu_e}\int_{-r}^{r}\frac{(h+z\tan\gamma)(r^2-z^2)^{1/2}}{[hk+(h+k)z\tan\gamma]^2} = 2n\varphi\Omega\sigma'_j hk^2\frac{1-\exp[-(\mu_i+\mu_e)L/\cos\gamma]}{\mu_i+\mu_e}I \ , \quad (2)$$

where the integral I represents a purely geometrical factor. The thickness L_a of the air interposed between scatterer and detector causes an attenuation such that the flux reaching the detector is $\Phi=\Phi_u\exp(-\mu_a L_a)$, with μ_a the attenuation coefficient of air for the radiation emerging from the scattering foil. Finally, the counting rate depends on the physical efficiency ϵ of the detector $N=\epsilon\Phi$. In the case of a planar high-purity Ge (HPGe) detector, when irradiation is restricted by collimation to its central region, the attenuation arises from the Be window of thickness L_B, from the dead layer, and from the collection volume of the Ge detector, the thicknesses of which are L_D and L_G, respectively. By denoting with μ_B and μ_G the attenuation coefficients of Be and Ge, the detector efficiency can be written

$$\epsilon=\exp[-(\mu_B L_B+\mu_G L_G)][1-\exp(-\mu_G L_G)] \ .$$

Then the differential cross section of the interaction of j type is given by

$$\sigma'_j=\frac{N}{2n\varphi\Omega hk^2 I\epsilon\exp[-(\mu_a L_a)]\{1-\exp[-(\mu_i+\mu_e)L/\cos\gamma]\}/(\mu_i+\mu_e)} \ .$$

φ and I are unsuitable for an accurate evaluation, the former because its measurement cannot be carried out directly at O, the latter because the finite dimension of the irradiated area of the detector gives rise to a penumbra ring on the scatterer with a consequent large indefiniteness of r value. This difficulty was overcome by measuring the counting rate of an interaction process having an accurately known cross section at 59.54 keV as the incoherent scattering in a very low atomic-number element such as Be. In this case, $\sigma'_j=\sigma'_I=\sigma'_{KN}S_{Be}$, where the Be scattering function S_{Be} is equal to four or only a few ten thousandths less in the considered interval $60°\leq\theta\leq120°$ (Ref. 1), and σ'_{KN} is the Klein-Nishina differential cross section. Then the differential cross section σ'_E for elastic scattering can be expressed simply in terms of the Klein-Nishina differential cross section. In fact, writing

$$\alpha=\rho\frac{1-\exp[-(\mu_i+\mu_e)L/\cos\gamma]}{\mu_i+\mu_e},$$

$$\beta=\epsilon\exp(-\mu_a L_a),$$

and observing that $n=\rho\mathcal{N}/M$, where $\mathcal{N}$ is the Avogadro number, M the atomic mass of the scattering atom, and ρ the density of the scatterer, the elastic differential cross section is given by

$$\sigma'_{Ex}=\sigma'_{KN}S_{Be}\frac{\alpha_{Be}\beta_{Be}M_x}{\alpha_x\beta_x M_{Be}}\frac{N_{Ex}}{N_{IBe}}. \quad (3)$$

Index x assigns the quantity to the generic scatterer and index Be to the Be scattering foil. N_E is the counting rate of elastic scattering events and N_I the counting rate of the incoherent ones.

III. EXPERIMENTAL PROCEDURE

The measurements carried out on foils of Al, V, Mo, Cd, and Pb covered three scattering angles, 60°, 90°, and 120°. In addition, the 90° series included Sn. At least three independent measurements were taken on each element and angle. Moreover, foils of two thicknesses were used for Al, Mo, and Sn. The different measurements on each element at each angle were carried out by alternating other elements and angles so that alignment had to be repeated at least twice for each geometric situation. Such a procedure performed by a proper goniometric irradiation bench equipped with a laser centering beam permitted the randomization of the uncertainties on the angle between source and detector axes and on the position of the scattering foil. The methodology adopted and the time of each measurement caused the total experiment to take almost two years, and in such a way the reproducibility of the results, too, underwent a severe test. Table I lists the properties of the scattering foils used.

TABLE I. Properties of the scattering foils. P, purity; $\mathcal{L}=\rho L$, mass thickness; $s_{\mathcal{L}}$ standard deviation of mass thickness on the whole irradiated area.

Element	P (%)	$\mathcal{L}$ (mg/cm^2)	$s_{\mathcal{L}}$ (mg/cm^2)
Be	99.8	103.30	0.26
Al	99.999	67.91	0.08
Al	99.999	130.70	0.11
V	99.8	77.05	0.20
Mo	99.9	107.30	0.41
Mo	99.9	238.27	0.32
Cd	99.99	211.35	0.48
Sn	99.99	94.38	0.37
Sn	99.99	174.52	0.67
Pb	99.99	143.43	0.92

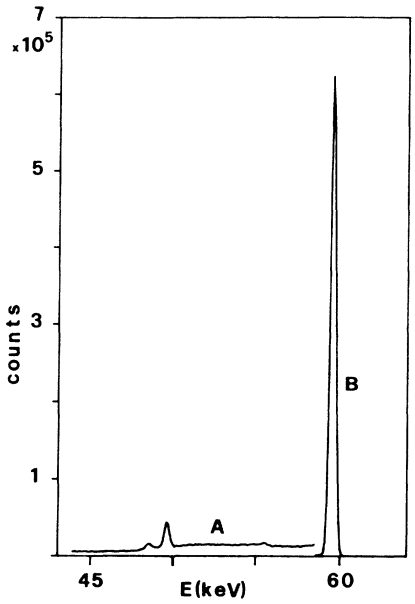

FIG. 2. Example of the response of the whole spectrometer to an ^{241}Am point source replacing the scatterer at the reference point O. Part A is scaled ten times with respect to the ordinate unit.

During each one of the repeated sets of measurements pertinent to each scattering angle, many observations of the background, i.e., of the spectral distribution obtained without scatterer, as well as many reference measurements with the Be foil, were carried out. The 59.54-keV primary photons were emitted from an ^{241}Am source of 18.5 GBq (0.5 Ci) and the instrumentation consisted of an HPGe planar detector 200 mm^2 in area and 10 mm in thickness combined with a 1024-channel spectrometer assisted by a double spectrum stabilizer. Both source and detector were more than 19 cm from the reference point O of the scatterer. The irradiated area of the detector was restricted to about 30 mm^2 by the collimator vane closest to it, the circular aperture of which was 6 mm in diameter. The working characteristics of the whole spectrometric instrumentation were very frequently checked throughout the period of the experiment by measuring its response to the radiation emitted by an ^{241}Am calibration point source placed at reference point O. An example of the results is shown in Fig. 2. This systematic check confirmed the high stability of the spectrometer.

IV. TREATMENT OF THE EXPERIMENTAL DATA

The counting rate of the Compton distribution from the Be scatterer and the rates of the elastic-scattering peaks from other elements pertinent to each angle were compared for each element after correction for background in order to evaluate whether, in terms of counting statistics, the amount of variability caused by the realignment was negligible. Since, on the whole, this test gave a significantly positive response, the counts for each element pertinent to the same angle were added up and were thought to be the result of a sole measurement, with a conservative standard deviation twice that of the counting statistics.

The values which were obtained in this manner for the Be scatterer were subsequently corrected for multiple scattering, double scattering, and mean tail ratio as derived from the response spectra, an example of which was shown in Fig. 2. In fact, that ratio strongly depends on the combination of detector and collimating system.[17] Of course, the counts in $K\alpha$ and $K\beta$ escape distributions were included in the main Compton distribution. The standard deviation of the counting statistics was the uncertainty index for the multiple-scattering value, while a maximum uncertainty equal to 10% of its calculated value was assigned to double scattering. The standard deviation of the mean seemed appropriate as the uncertainty index of the tail ratio, the mean value of which was 1.0325 over about 20 measurements. The experimental results of the other scattering foils were corrected at first for the counts due to the Compton distribution, keeping in mind the discontinuities caused in the latter by the binding energy of K, L, and M electrons,[18] and the possible distortion produced in it by the higher-energy part of the double-scattering distribution, and then for the K escape, as given by the Axel model.[19] The maximum relative uncertainties assigned to these corrections were 25% and 10%, respectively. This procedure provided the values of the quantities $N_{I\mathrm{Be}}$ and N_{Ex} of Eq. (3).

In order to have better values and to randomize them, the factors α_x, β_x and $\alpha_{\mathrm{Be}}, \beta_{\mathrm{Be}}$ were evaluated for each experimental situation by means of the attenuation coefficients taken from four independent sources: (i) the tabulation of McMaster *et al.*,[20] (ii) the tabulation of Veigele,[21] (iii) the calculations of Storm and Israel,[22] and (iv) the calculations of Scofield[23] combined with those of Hubbell *et al.*[1] Moreover, the uncertainty on α_x, β_x, α_{Be}, and β_{Be}, to be attributed to the standard deviation in scatterer thickness, was appropriately added in quadrature to the one coming from the uncertainty in attenuation coefficients. The use in some cases of two different thicknesses was suggested by the opportunity of comparing also results where the variability of either thickness or attenuation coefficients prevails. In fact, by defining $f=1-\exp[-(\mu_i+\mu_e)L/\cos\gamma]$, it is $\alpha=\rho L\,(\cos\gamma)^{-1}$ for $f\approx 0$ and $\alpha=\rho(\mu_i+\mu_e)^{-1}$ for $f\approx 1$. Thus the evaluation of the attenuation coefficients becomes critical in some cases, and their formation must be carried out with great care. Therefore, keeping in mind the geometry used, the coherent scattering coefficient was excluded for the beam incident on and included for the beam emerging from the scatterer. Once more with reference to Eq. (3), the uncertainties on the Klein-Nishina cross section and on the atomic masses were assumed to be zero and negligible, respectively.

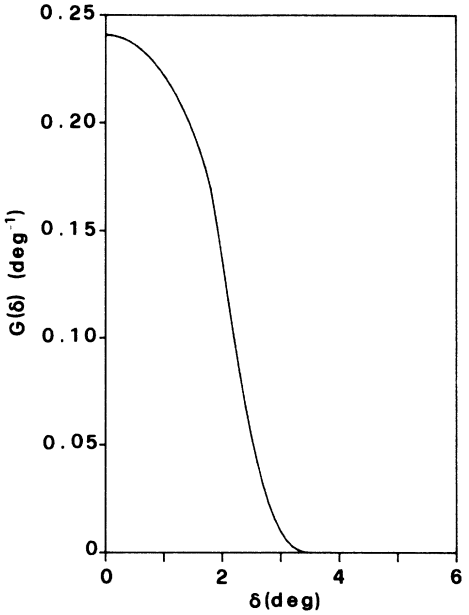

FIG. 3. Distribution of the calculated angular response function for the present experiment.

Finally, a very small correction is needed. Equation (1) and consequently Eq. (2) were obtained for very small, or, rather, for a point source. As a matter of fact, the source is finite, as is the detector-irradiated area, and thus a finite, even if small, angle of dispersion is present. Figure 3 shows the response function $G(\delta)$ normalized to the unitary integral area as it was calculated around the nominal scattering angle for the present arrangement. The dispersion may be seen as rather small, so that as a good approximation it can be accounted for by considering the differential cross sections in Eq. (2) as mean values

$$\overline{\sigma'_j}=\frac{\int_{-\delta_m}^{\delta_m}\sigma'_j(\theta+\delta)G(\delta)d\delta}{\int_{-\delta_m}^{\delta_m}G(\delta)d\delta}=\int_{-\delta_m}^{\delta_m}\sigma'_j(\theta+\delta)G(\delta)d\delta\ ,$$

where δ_m is the maximum dispersion angle. The ratio of the cross section for an angle to the mean around it can easily be calculated for theoretical values by using the data of Kane *et al.*[7] and Kissel[5,24] for elastic scattering and the Klein-Nishina formula for Compton scattering. Such results were assumed to be valid also for experimental data.

V. EXPERIMENTAL RESULTS AND DISCUSSION

Table II lists the values of the differential cross section of elastic scattering σ'_E obtained by the present experiment together with their relative s_r and absolute s_E stan-

TABLE II. Differential cross section of elastic scattering at 59.54 keV. Numbers in square brackets denote powers of 10.

Element	Z	θ (deg)	σ'_E (b/sr)	s_r (%)	s_E (b/sr)	σ'_K (b/sr)	s_K (b/sr)
Al	13	60	0.4956[−1]	1.30	0.64[−3]	0.511[−1]	0.10[−2]
V	23		0.1704	1.15	0.20[−2]	0.177	0.35[−2]
Mo	42		1.306	1.00	0.13[−1]	1.33	0.27[−1]
Cd	48		1.679	1.00	0.17[−1]	1.70	0.34[−1]
Pb	82		6.882	1.00	0.69[−1]	6.85	0.13
Al	13	90	0.1633[−1]	2.15	0.35[−3]	0.165[−1]	0.33[−3]
V	23		0.633[−1]	2.10	0.13[−2]	0.648[−1]	0.13[−2]
Mo	42		0.5030	1.25	0.63[−2]	0.500	0.10[−1]
Cd	48		0.7508	1.25	0.94[−2]	0.748	0.15[−1]
Sn	50		0.8259	1.15	0.95[−2]	0.824	0.16[−1]
Pb	82		2.343	1.15	0.27[−1]	2.27	0.45[−1]
Al	13	120	0.966[−2]	4.60	0.44[−3]	0.971[−2]	0.19[−3]
V	23		0.563[−1]	2.55	0.14[−2]	0.578[−1]	0.12[−2]
Mo	42		0.3376	1.45	0.49[−2]	0.341	0.68[−2]
Cd	48		0.5650	1.40	0.79[−2]	0.573	0.11[−1]
Pb	82		1.485	1.35	0.20[−1]	1.44	0.29[−1]

dard deviations. The relative standard deviation appreciably exceeds 2% in one case only, whereas for most it is well below that value. As a check, the same cross sections were evaluated with reference to the incoherent scattering of Al foils. The agreement for each element at each angle was largely within the quoted uncertainty. In the same table the corresponding values σ'_K calculated by Kane *et al.*[7] and by Kissel[5,24] are quoted, as well as their absolute uncertainty s_K evaluated on the 2% basis suggested by Kane *et al.*[7]

If each calculated value is regarded as a mean and its uncertainty as the standard deviation of that mean, then t test can be used to compare experimental and theoretical individual data. Such a test shows that each difference between each pair of values in the mean could arise by chance considerably more often than once in 20 times. Therefore, it is unlikely that there is any significant difference between the values of each such pair.[25] Figure 4 represents the available experimental data of the elastic differential cross section normalized to the values predicted by Kane *et al.*[7] and Kissel[5,24] as a function of the atomic number Z for the three angles considered in the

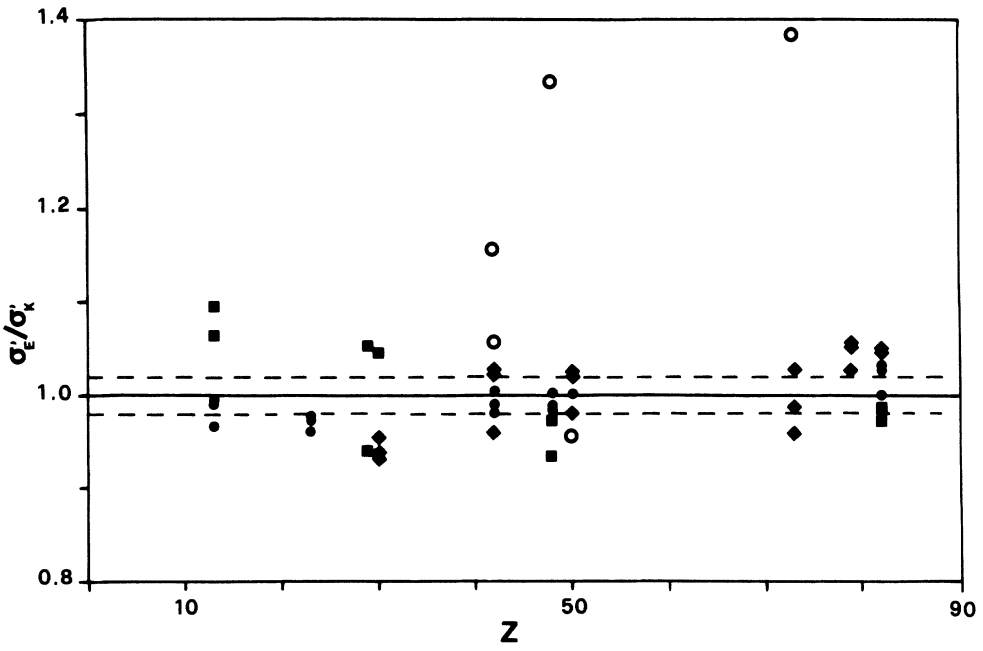

FIG. 4. Various authors' experimental values of the elastic scattering cross section normalized to the predictions of the calculation procedure of Kissel and co-workers at 60°, 90°, and 120° scattering angles. ●, present work; ♦, Schumacher and Stoffregen (Ref. 9); ■, Eichler and de Barros (Ref. 10); ○, Nandi *et al.* (Ref. 11).

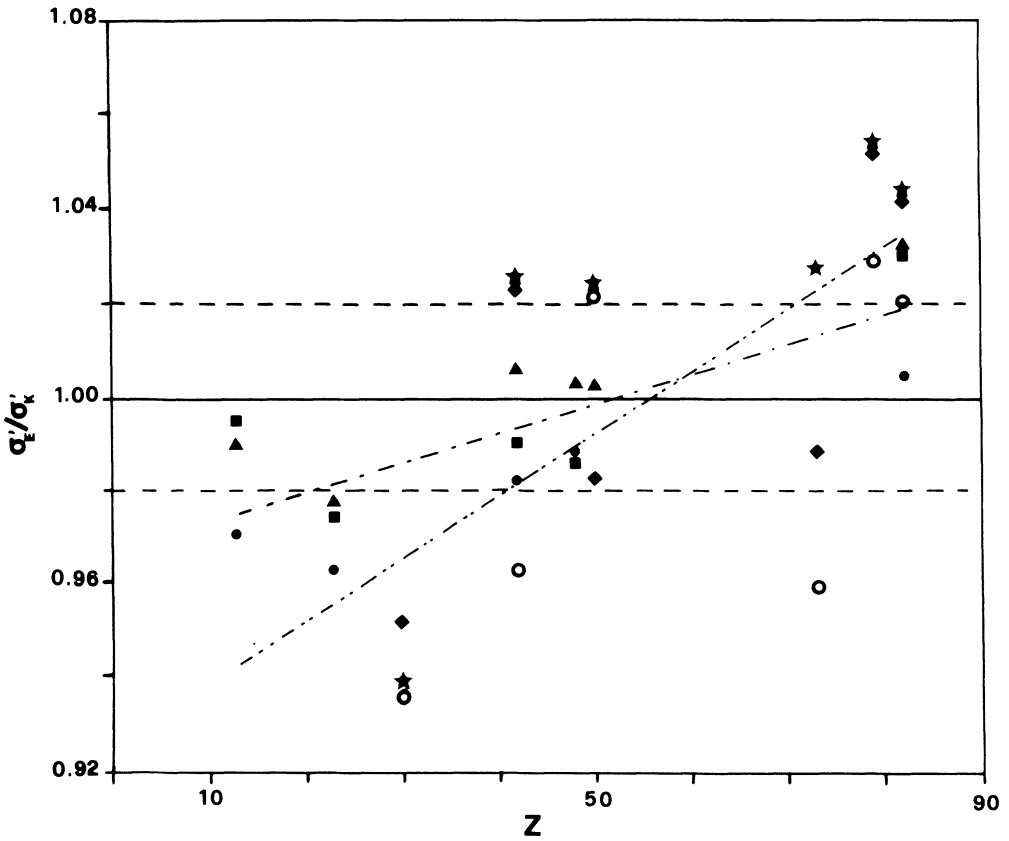

FIG. 5. Values of the present work and values of Schumacher and Stoffregen (Ref. 9) normalized to the prediction of the calculation procedure of Kissel and co-workers. Present work: ●, 60°; ▲, 90°; and ■, 120° scattering angles. Schumacher and Stoffregen: ○, 60°; ★, 90°; and ♦, 120° scattering angles. —·—·—·, straight line interpolating the present values; ——··—— straight line interpolating the Schumacher and Stoffregen values.

present work. It is noteworthy that the results obtained by the present work have a small dispersion, always below $\pm 1.5\%$, with the scattering angle. Figure 5 shows the same values restricted to the present data and to those of Schumacher and Stoffregen.[9] The larger scale of ordinates permits the use of a different mark for each angle. Both the groups of values were interpolated by straight lines, also shown in the drawing. Even if the deviation from unity of each value has a high probability not to be statistically significant, the fact that both straight lines present positive slopes is noteworthy, as is the fact that the values at 60° were lower than those at the other two angles almost systematically. Both these facts could be due to chance or to some undetected experimental artifact, but it seems appropriate to call attention to them for future accurate measurements of elastic differential cross sections.

VI. CONCLUSIONS

The small uncertainties in the values obtained by the present work for the differential cross section of elastic scattering of photons on atoms make it possible to validate the values calculated by the method of Kissel and co-workers with confidence, at least at a photon energy of 59.54 keV and in the scattering interval $60° \leq \theta \leq 120°$. These results, together with those given by other authors for other energies and angles, point out the usefulness of making available tabulations, based on the calculation procedure of Kissel and co-workers, thickened in the grids of both energies and elements, together with practical and accurate interpolating functions.

ACKNOWLEDGMENTS

The authors wish to thank Dr. L. Kissel and Mr. J. H. Hubbell for their kindness in supplying theoretical data. Special thanks to Dr. G. Frazzoni for his invaluable aid in designing the irradiation bench. The authors are also grateful to Ministero della Pubblica Istruzione (Rome) and to Istituto Nazionale di Fisica Nucleare (Rome) for their financial support.

[1]J. H. Hubbell, W. J. Veigele, E. A. Briggs, R. T. Brown, D. T. Cromer, and R. J. Howerton, J. Phys. Chem. Ref. Data **4**, 471 (1975); **6**, 615(E) (1977).

[2]J. H. Hubbell and I. Øverbø, J. Phys. Chem. Ref. Data **8**, 69 (1979).

[3]D. Schaupp, M. Schumacher, F. Smend, P. Rullhusen, and J. H. Hubbell, J. Phys. Chem. Ref. Data **12**, 467 (1983).

[4]L. Kissel, R. H. Pratt, and S. C. Roy, Phys. Rev. A **22**, 1970 (1980).

[5]L. Kissel, Sandia National Laboratories Report No. SANT 84-0294, 1984 (unpublished).

[6]L. Kissel and R. H. Pratt, in *Atomic Inner-Shell Physics,* edited by B. Crasemann (Plenum, New York, 1985).

[7]P. P. Kane, L. Kissel, R. H. Pratt, and S. C. Roy, Phys. Rep. **140**, 75 (1986).

[8]D. A. Bradley and A. M. Ghose, Phys. Med. Biol. **29**, 1385 (1984).

[9]M. Schumacher and A. Stoffregen, Z. Phys. A **283**, 15 (1977).

[10]J. Eichler and S. de Barros, Phys. Rev. A **32**, 789 (1985).

[11]S. S. Nandi, R. Dutta, and N. Chaudhuri, J. Phys. B **20**, 4027 (1987).

[12]F. Smend and H. Czerwinski, Z. Phys. D **1**, 139 (1986).

[13]C. Bui and M. Milazzo, Nuovo Cimento D **11**, 655 (1989).

[14]K. M. Varier and M. P. Unnikrishnan, Nucl. Instrum. Methods A **280**, 428 (1989).

[15]A. L. Hanson, G. E. Gigante, and M. Meron, Phys. Rev. Lett. **61**, 135 (1988); A. L. Hanson and G. E. Gigante, Phys. Rev. A **40**, 171 (1989).

[16]D. A. Bradley and A. M. Ghose, Phys. Rev. A **33**, 191 (1986).

[17]S. O. Manninen, M. J. Cooper, and D. A. Cardwell, Nucl. Instrum. Methods A **245**, 485 (1986).

[18]A. Sommerfeld, Phys. Rev. **50**, 38 (1936); S. Manninen, N. G. Alexandropoulos, and M. J. Cooper, Philos. Mag. B **52**, 899 (1985).

[19]P. Axel, Brookhaven National Laboratory Report No. BNL 271 (1953) (unpublished).

[20]W. H. McMaster, N. K. Del Grande, J. H. Mallett, and J. H. Hubbell, Lawrence Livermore Laboratory Report No. UCRL 50174, Section II, Rev. 1 (1969) (unpublished).

[21]W. J. Veigele, At. Data **5**, 51 (1973).

[22]E. Storm and H. I. Israel, Nucl. Data. Tables A **7**, 565 (1970).

[23]J. H. Scofield, Lawrence Livermore Laboratory Report No. UCRL 51326 (1973) (unpublished).

[24]L. Kissel (private communication).

[25]P. J. Campion, J. E. Burns, and A. Williams, *A Code of Practice for the Detailed Statement of Accuracy* (National Physical Laboratory, London, 1973).